

Experimental Detection on Thickness Fluctuation of In_xGa_{1-x}As-Based Indium-Rich Cluster Structure

Yanting Kong, Rong Ma, Bin Shen, and Qingnan Yu 

Abstract—The thickness detection of quantum well has always been the research focus, especially for In_xGa_{1-x}As-based indium-rich cluster (IRC) structure, which has a thickness fluctuation of normal and indium-deficient InGaAs layers caused by IRC effect. In this paper, a simple and effective detection method for the special IRC structure is proposed by point-to-point acquisition. The photoluminescence (PL) spectra emitted from different In_xGa_{1-x}As positions are measured by moving the metal mask with a 0.2-mm-diameter light hole. By establishing the relationship between In_xGa_{1-x}As thickness and spectral intensity, the thickness fluctuation of normal In_{0.17}Ga_{0.83}As and indium-deficient In_{0.12}Ga_{0.88}As layers is determined by comparing the intensity of dual peaks. The dual peaks are typical feature of this IRC structure, which is caused by the migration of indium atoms. The significance of this experimental results is that it not only can detect the thickness distribution of In_xGa_{1-x}As materials with different x values, but also determine the critical thickness of indium atom migration in the growth of highly strained quantum well.

Index Terms—InGaAs, indium-rich cluster, indium atom migration, thickness distribution.

I. INTRODUCTION

IT HAS been well known that conventional InGaAs/GaAs semiconductor lasers are playing an important role in many application fields [1], [2], [3], [4], [5], [6]. They have a quasi-rectangle well structure, in which each well consists of a fixed indium content and strain type in material system. Recently, we reported a special InGaAs-based indium-rich cluster (IRC) structure containing variable indium contents and thicknesses in an In_xGa_{1-x}As/GaAs system. It can produce some interesting changes that favor the development of new types of lasers

Manuscript received 10 October 2022; accepted 13 October 2022. Date of publication 17 October 2022; date of current version 2 November 2022. This work was supported in part by the National Natural Science Foundation of China under Grant 62204172, in part by the Natural Science Foundation of the Jiangsu Higher Education Institutions of China under Grant 22KJB140016, in part by the Shuangchuang Ph.D award in Jiangsu province (from World Prestigious Universities) under Grant JSSCBS-20210870, in part by the Startup Foundation for Introducing Talent of NUIST Binjiang College under Grant 550221009, in part by the Anhui Province Key Laboratory of Optoelectric Materials Science and Technology under Grant OMST202105, and in part by the 14th Five-Year Jiangsu Provincial Key Discipline Construction Project-Electronic Science and Technology under Grant 161. (*Corresponding author:* Qingnan Yu)

Yanting Kong, Rong Ma, and Bin Shen are with the School of Electronic Information Engineering, Wuxi University, Wuxi 214105, China (e-mail: 369212726@qq.com; 3281680665@qq.com; s18914110528@163.com).

Qingnan Yu is with the School of Electronic Information Engineering, Wuxi University, Wuxi 214105, China, and also with the Anhui Province Key Laboratory of Optoelectric Materials Science and Technology, Anhui Normal University, Wuhu 241000, China (e-mail: yuqingnan1@126.com).

Digital Object Identifier 10.1109/JPHOT.2022.3215276

[7], [8]. This structure is associated with the IRC effect, in which the IRCs were commonly regarded as a sort of defect to avoid for the conventional InGaAs quantum well structure so that its special optical characteristics were neglected in the past [9]. The fundamental principle of the IRC formation is that in the growth process of an In_xGa_{1-x}As/GaAs quantum structure, indium atoms would migrate upward to the surface along the material growth direction and form many clusters on the surface of the In_xGa_{1-x}As material to relax high strain in the In_xGa_{1-x}As layer after the In_xGa_{1-x}As is grown to exceed a few mono-layers on the GaAs layer [10]. Since the migration of indium atoms reduces the indium contents in the corresponding InGaAs regions, which are close to the upper surface of the InGaAs layer, the indium-deficient InGaAs region is generated and distributed in the growth directions. How to evaluate the thicknesses fluctuation of normal and indium-deficient In_xGa_{1-x}As layers has become a research difficulty in the study of the IRC structure.

Nowadays, there are some techniques to obtain effective detection data for conventional quantum well structure, such as atom probe tomography [11], X-ray dual crystal diffraction [12], [13] and theoretical simulation [14]. However, the expensive experimental equipment or inaccurate simulation results make it difficult to popularize, especially for In_xGa_{1-x}As-based indium-rich cluster (IRC) structure. The formation mechanism of this IRC structure is complex because it involves the migration of indium atoms, strain accumulation, stress release, lattice mismatch, mixed strain, etc., which will make it difficult to describe IRC effect accurately by theoretical calculation. Similarly, it is inconvenient for most scientific researchers to use expensive equipment for experimental detection. Therefore, in order to determine the thickness fluctuation of normal and indium-deficient In_xGa_{1-x}As layers in indium-based IRC active layer, a simple and effective detection method is proposed by point-to-point acquisition.

Hence, in this letter, the asymmetrical IRC structure is first grown. Then the spontaneous emission spectra are collected from the bottom of the chip by point-to-point measurement with a movable metal mask. Finally, the thickness distribution of In_xGa_{1-x}As materials with different x values in IRC structure are determined by establishing the relationship between active layer thickness and spectral intensity. In addition, the threshold thickness of indium atom migration in highly strained indium-based quantum confined structure is also obtained.

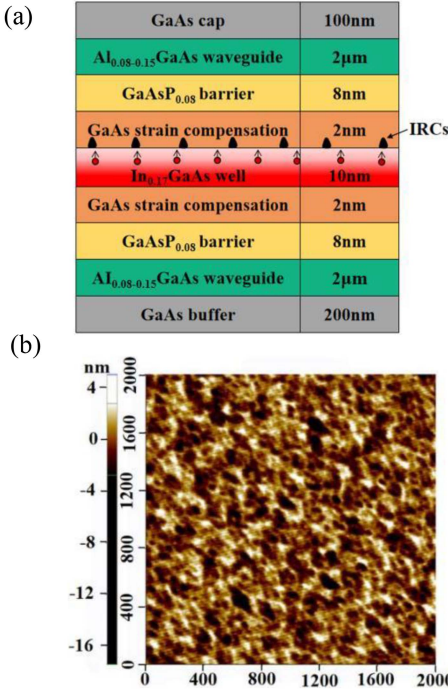


Fig. 1. (a) InGaAs-based IRC structure. (b) AFM image of IRCs on InGaAs surface.

II. IRC STRUCTURE AND EXPERIMENTAL SETUP

For the experimental measurement, the InGaAs-based IRC structure with the thickness accuracy of 0.1 nm is grown on the GaAs (001) substrate by metal organic chemical vapor deposition (MOCVD) (Germany Aixtron Co., Ltd., model aix200/4), as shown in Fig. 1(a). The size of the device is designed to be 1.5 mm in width and 3.0 mm in length. In order to generate enough strain accumulation and IRC effect [13], [15], [16], the original active layer is In_{0.17}Ga_{0.83}As materials with a thickness of 10 nm here. The thinner InGaAs layer and a lower x-value in In_xGa_{1-x}As is not enough to obtain IRC effect because of the lower strain accumulation and lattice mismatching [17]. The In_{0.17}Ga_{0.83}As material is sandwiched by 2-nm-thick GaAs compensation layers. Beyond the GaAs compensation layers are the 8-nm-thick GaAsP_{0.08} barriers. The sample was deposited at a rate of 0.75 μm/h and 100 mbar pressure under 660 °C. The high temperature of 660 °C was applied to increasing the migration length of the indium atoms and is beneficial to the formation of IRCs in the material growth. The V/III ratio was 40 for the structure growth. In order to prove that the InGaAs sample contains IRC effect, the surface topography of InGaAs quantum structure is measured and characterized. Fig. 1(b) shows an image of the clusters obtained by using atomic force microscopy (AFM) (Park Systems Instrument Co., Ltd., model XE100). The IRC existence on the InGaAs surface can be confirmed.

According to our previous research, the asymmetrical IRC structure mainly includes normal In_{0.17}Ga_{0.83}As layer and indium-deficient In_{0.12}Ga_{0.88}As layer, which is caused by indium atom migration due to the higher strain accumulation [7]. The migration and accumulation of indium atoms along the growth direction would reduce the indium content in

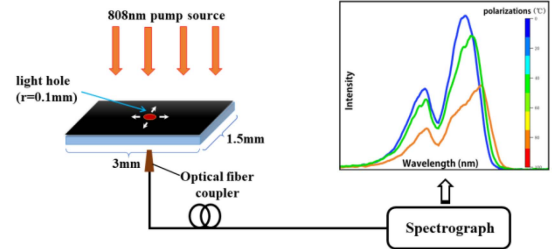


Fig. 2. Experimental setup for PL measurement with a metal mask.

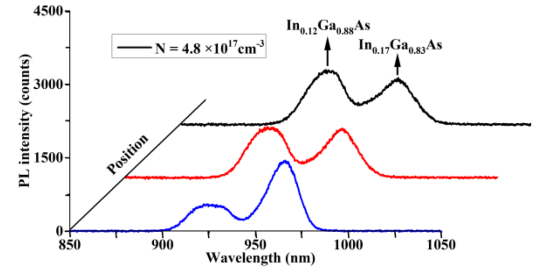


Fig. 3. The PL spectra measured from different locations of IRC device.

corresponding In_xGa_{1-x}As region and form indium-deficient In_{0.12}Ga_{0.88}As layer. In order to calculate the thickness distribution of In_{0.17}Ga_{0.83}As and In_{0.12}Ga_{0.88}As materials, the experimental system is established, as shown in Fig. 2. The IRC sample was processed into an in-plane configuration of 3 mm × 1.5 mm in size. The device is vertically pumped from fiber-coupled 808 nm pulsed laser under room temperature. In order to improve accuracy, the pulse width was set to 20 ms to eliminate the influence of thermal effect on spectral intensity. The pump beam is reshaped from Gaussian pattern to flat-top one to generate fixed carrier distribution within the pumped region. A removable mask with 0.2-mm-diameter hole was covered on the upper surface of the sample. The transparent hole in mask is used to select a fixed pumping region. The fiber coupler is placed on the lower surface of the sample and aligned with the light hole to collect the photoluminescence (PL) spectra emitted from the corresponding pumping region. By moving the metal mask with the transparent hole to select different pumping area, the PL spectra from different positions throughout the whole IRC sample are measured one by one. The size of the small hole represents the pump area and the measurement division.

III. RESULTS AND ANALYSIS

Fig. 3 shows the PL spectra emitted from three different locations of In_xGa_{1-x}As IRC sample under the injected-carrier density of $N = 4.8 \times 10^{17} \text{ cm}^{-3}$, which are obtained by moving the metal mask with light hole. The dual peaks appear clearly in each PL spectrum, which differs from the single-peak emission spectrum generated from a conventional quantum well. The dual-peak configuration in the PL spectra is a remarkable feature of the IRC effect taking place in the InGaAs-based quantum confined structure. The PL spectra in Fig. 3 cover the range from 900 nm to 1000 nm, which corresponds to the range of

photon energy from 1.24 to 1.38 eV. However, the band gaps of GaAs, $\text{Al}_{0.08-0.15}\text{GaAs}$ and $\text{GaAsP}_{0.08}$ materials composing the structure are 1.424 eV, 1.52–1.61 eV and 1.53 eV, respectively. These materials do not contribute to the PL spectra ranging from 900 nm to 1000 nm. Therefore, the background radiation does not interfere with the measurement results. It is noticed that since indium-rich clusters consist of indium atoms or InAs compounds rather than InGaAs materials, these clusters do not contribute to the PL spectra ranging from 900 to 1000 nm because the unstrained InAs compound has a band gap of 0.35 eV, which corresponds to the emission wavelength of 3.5 μm , and the compressively strained InAs/GaAs quantum dots produce an emission with a peak wavelength of 1.3 μm due to a large lattice mismatch [18], [19]. Therefore, the particular feature with two peaks is attributed to all emissions from normal $\text{In}_{0.17}\text{Ga}_{0.83}\text{As}$ layer and indium-deficient $\text{In}_{0.12}\text{Ga}_{0.88}\text{As}$ layer. The spectral peak on the right in Fig. 3 is emitted from $\text{In}_{0.17}\text{Ga}_{0.83}\text{As}$ material, which has a narrow band gap. The left peak in Fig. 3 is emitted from $\text{In}_{0.12}\text{Ga}_{0.88}\text{As}$ material, which has a wide band gap. Because the photon energies emitted from $\text{In}_{0.17}\text{Ga}_{0.83}\text{As}$ and $\text{In}_{0.12}\text{Ga}_{0.88}\text{As}$ layers are distinct, the thickness distribution of that can be determined by analyzing the intensity of dual peaks in Fig. 3.

The relationship between spectral intensity and the thickness of $\text{In}_x\text{Ga}_{1-x}\text{As}$ well can be established by the following approach [20].

$$P = (\gamma BN^2hcSL) / \left[n\lambda_{PL}(1 - R_1R_2)^2 \right] \quad (1)$$

where P is the PL spectral intensity, L denotes the thickness of active layer, γ is the quantum efficiency, which can be estimated by $\lambda_{\text{pump}}/\lambda_{\text{PL}}$, B is bimolecular recombination coefficient, which is $1.0 \times 10^{-10} \text{ cm}^{-3}/\text{sec}$ [21], N denotes carrier density, h is the Planck constant, c is the speed of light, S denotes the area of IRC device, R_1 and R_2 are the reflectivity of the dual facets, which are determined by the GaAs material index [22], n is the refractive index of $\text{In}_x\text{Ga}_{1-x}\text{As}$, which mainly depends on the indium content x . The difference of relative refractive index between $\text{In}_{0.17}\text{Ga}_{0.83}\text{As}$ and $\text{In}_{0.12}\text{Ga}_{0.88}\text{As}$ materials is just 0.002 [23], [24]. Therefore, the parameters B , N , h , c , S , R_1 , R_2 and n in (1) can be regarded as constants.

According to the (1), the PL intensity mainly depends on the $\text{In}_x\text{Ga}_{1-x}\text{As}$ material thickness L and the peak wavelength λ_{PL} . Based on the Fig. 3, the peak wavelengths λ_{PL} of $\text{In}_{0.17}\text{Ga}_{0.83}\text{As}$ and $\text{In}_{0.12}\text{Ga}_{0.88}\text{As}$ are 965 nm and 925 nm. Therefore, the thickness distribution of normal $\text{In}_{0.17}\text{Ga}_{0.83}\text{As}$ and indium-deficient $\text{In}_{0.12}\text{Ga}_{0.88}\text{As}$ materials can be calculated by comparing the intensities of dual peaks in Fig. 3. Based on the total $\text{In}_x\text{Ga}_{1-x}\text{As}$ thickness of 10 nm, the thickness fluctuation of normal $\text{In}_{0.17}\text{Ga}_{0.83}\text{As}$ layer and indium-deficient $\text{In}_{0.12}\text{Ga}_{0.88}\text{As}$ layer is calculated and shown in Fig. 4(a).

It is clearly observed that the thickness distribution of $\text{In}_{0.17}\text{Ga}_{0.83}\text{As}$ and $\text{In}_{0.12}\text{Ga}_{0.88}\text{As}$ materials varies at different locations. This is because the migration of indium atoms will lead to nonuniform strain accumulation and distribution. This would produce different degrees of IRC effect and form discrete

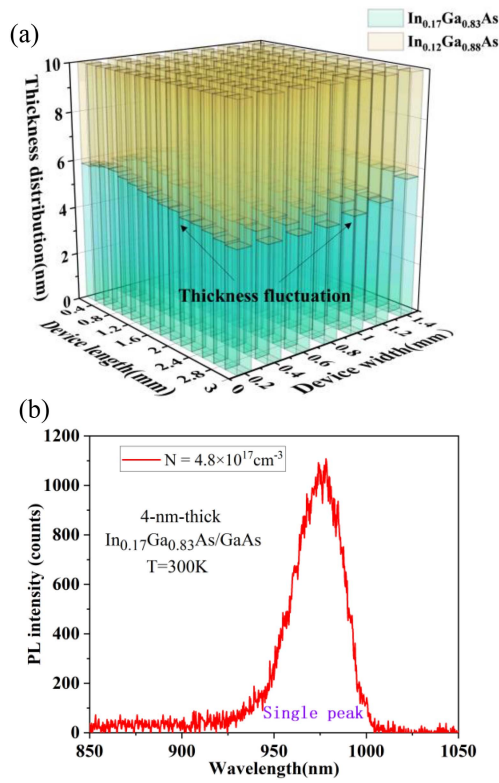


Fig. 4. (a) Thickness distribution of normal $\text{In}_{0.17}\text{Ga}_{0.83}\text{As}$ and indium-deficient $\text{In}_{0.12}\text{Ga}_{0.88}\text{As}$ materials. (b) The PL spectrum measured from a 4-nm-thick $\text{In}_{0.17}\text{Ga}_{0.83}\text{As/GaAs}$ compressively strained quantum well.

IRCs with different sizes, as shown in Fig. 1(b). It leads to thickness fluctuation of $\text{In}_{0.17}\text{Ga}_{0.83}\text{As}$ and $\text{In}_{0.12}\text{Ga}_{0.88}\text{As}$ materials. Fig. 4(a) also shows that the indium-deficient $\text{In}_{0.12}\text{Ga}_{0.88}\text{As}$ material is located on the upper surface of normal $\text{In}_{0.17}\text{Ga}_{0.83}\text{As}$ layer along the growth direction. This is caused by the migration of indium atoms upward to the surface when the $\text{In}_{0.17}\text{Ga}_{0.83}\text{As}$ is grown to exceed a few mono-layers on the GaAs, as shown in Fig. 1(a). In addition, the thickness fluctuation of normal $\text{In}_{0.17}\text{Ga}_{0.83}\text{As}$ layer ranges from 4 to 6 nm in Fig. 4(a). The result reveals that the threshold thickness of indium atom migration can be estimated as 4 nm according to Fig. 4(a). It means that the migration of indium atoms will not occur as long as the thickness of $\text{In}_{0.17}\text{Ga}_{0.83}\text{As}$ layer does not exceed 4 nm. This is because the smaller strain accumulation is not enough to produce IRC effect until the $\text{In}_{0.17}\text{Ga}_{0.83}\text{As}$ thickness exceeds the critical thickness of 4 nm. In order to demonstrate the accuracy of this measurement method, the PL spectrum of a 4-nm-thick $\text{In}_{0.17}\text{Ga}_{0.83}\text{As/GaAs}$ compressively strained quantum well with the thickness accuracy of 0.1 nm under a same injected-carrier density is measured. The result is shown in Fig. 4(b).

Compared with the results in Fig. 3, there is only one peak in the PL spectrum under the same injected-carrier density of $N = 4.8 \times 10^{17} \text{ cm}^{-3}$, as shown in Fig. 4(b). This result indicates that indium atoms do not migrate to form IRCs in the 4-nm-thick $\text{In}_{0.17}\text{Ga}_{0.83}\text{As/GaAs}$ material. Although there is strain accumulation in $\text{In}_{0.17}\text{Ga}_{0.83}\text{As}$ material, it is not enough to produce IRC

effect. The spectral feature with dual peaks disappears. In order to further prove the accuracy of this method, the reference 25 is cited, where the PL spectrum of an $\text{In}_{0.15}\text{Ga}_{0.85}\text{As}/\text{GaAs}$ material with a thickness of more than 6 nm shows two peaks caused by IRC effect [25]. It can be evaluated that the PL spectrum of an $\text{In}_{0.17}\text{Ga}_{0.83}\text{As}/\text{GaAs}$ material with a thickness of more than 4 nm should be two peaks. The analysis is consistent with the experimental results, which demonstrates the relatively accuracy of this measurement method. Therefore, the work is significant to detect the characteristics of IRC structure, because it not only can detect the thickness fluctuation of normal $\text{In}_{0.17}\text{Ga}_{0.83}\text{As}$ and indium-deficient $\text{In}_{0.12}\text{Ga}_{0.88}\text{As}$ materials, but also determine the critical thickness of indium atom migration in the growth of highly strained quantum well.

IV. CONCLUSION

In conclusion, we proposed a simple and effective detection method for the asymmetric InGaAs-based IRC structure by point-to-point scanning measurement. The PL spectra emitted from different $\text{In}_x\text{Ga}_{1-x}\text{As}$ positions are collected by moving the metal mask with a 0.2-mm-diameter light hole. The thickness fluctuation of normal $\text{In}_{0.17}\text{Ga}_{0.83}\text{As}$ layer and indium-deficient $\text{In}_{0.12}\text{Ga}_{0.88}\text{As}$ layer is obtained by comparing the intensity of dual peaks in PL spectra. The experimental result is significant because it not only can calculate the thickness distribution of $\text{In}_{0.17}\text{Ga}_{0.83}\text{As}$ and $\text{In}_{0.12}\text{Ga}_{0.88}\text{As}$ materials, but also determine the critical thickness of indium atom migration. This method has important research value for the development of $\text{In}_x\text{Ga}_{1-x}\text{As}$ -based IRC structures as well as strained quantum wells with high quality.

IV. DISCLOSURES

The authors declare no conflicts of interest.

IV. DATA AVAILABILITY

Data underlying the results presented in this paper are not publicly available at this time but may be obtained from the authors upon reasonable request.

REFERENCES

- [1] F. Zubov et al., "Improved performance of InGaAs/GaAs microdisk lasers epi-side down bonded onto a silicon board," *Opt. Lett.*, vol. 46, no. 16, pp. 3853–3856, Jul. 2021.
- [2] C. Gmachl, D. L. Sivco, R. Colombelli, F. Capasso, and A. Y. Cho, "Ultra-broadband semiconductor laser," *Nature*, vol. 21, pp. 883–887, Feb. 2002.
- [3] P. Wang, P. Tayebati, D. Vakhshoori, C. Lu, and M. Azimi, "Half-symmetric cavity microelectromechanically tunable vertical cavity surface emitting lasers with single spatial mode operating near 950 nm," *Appl. Phys. Lett.*, vol. 75, no. 7, pp. 897–898, Apr. 1999.
- [4] F. Li et al., "Tunable high-power high-brightness linearly polarized vertical-external-cavity surface-emitting lasers," *Appl. Phys. Lett.*, vol. 88, no. 2, Jan. 2006, Art. no. 021105.
- [5] Q. W. Wang, J. Li, J. Y. Lin, and H. X. Jiang, "Stability and nucleation of IR_n ($n = 1–5$) clusters on different $\gamma\text{-Al}_2\text{O}_3$ surfaces: A density functional theory study," *Phys. Lett. A.*, vol. 380, no. 5, pp. 718–725, Jan. 2016.
- [6] T. Butler et al., "Optical ultrafast random number generation at 1 Tb/s using a turbulent semiconductor ring cavity laser," *Opt. Lett.*, vol. 41, no. 2, pp. 388–391, Jan. 2016.
- [7] Q. Yu et al., "InGaAs-based well-island composite quantum-confined structure with superwide and uniform gain distribution for great enhancement of semiconductor laser performance," *ACS Photon.*, vol. 5, no. 12, pp. 4896–4902, Nov. 2018.
- [8] Q. Yu et al., "Quantum confined indium-rich cluster lasers with polarized dual-wavelength output," *ACS Photon.*, vol. 6, no. 8, pp. 1990–1995, Jul. 2019.
- [9] A. Jasik et al., "The influence of the growth temperature and interruption time on the crystal quality of InGaAs/GaAs QW structures grown by MBE and MOCVD methods," *J. Cryst. Growth*, vol. 310, no. 11, pp. 2785–2792, May 2008.
- [10] D. Schlenker, T. Miyamoto, Z. Chen, F. Koyama, and K. Iga, "Growth of highly strained GaInAs/GaAs quantum wells for 1.2 μm wavelength lasers," *J. Cryst. Growth*, vol. 209, no. 1, pp. 27–36, Jan. 2000.
- [11] S. E. Bennett et al., "Atom probe tomography assessment of the impact of electron beam exposure on $\text{In}_{x}\text{Ga}_{1-x}\text{N}/\text{GaN}$ quantum wells," *Appl. Phys. Lett.*, vol. 99, no. 2, Jul. 2011, Art. no. 021906.
- [12] K. Yuan, K. Radhakrishnan, H. Q. Zheng, Q. D. Zhuang, and G. I. Ing, "Characterization of linearly graded metamorphic InGaP buffer layers on gaas using high-resolution X-ray diffraction," *Thin Solid Films*, vol. 391, no. 1, pp. 36–41, Jul. 2001.
- [13] C. Ferrari, M. R. Bruni, F. Martelli, and M. G. Simeone, "InGaAs/GaAs strained single quantum well characterization by high resolution X-ray diffraction," *J. Cryst. Growth*, vol. 126, no. 1, pp. 144–150, Jan. 1993.
- [14] T. J. Yang, R. Shivaraman, J. S. Speck, and Y. R. Wu, "The influence of random indium alloy fluctuations in indium gallium nitride quantum wells on the device behavior," *J. Appl. Phys.*, vol. 116, no. 11, Sep. 2014, Art. no. 131104.
- [15] S. J. Ma, Y. Wang, H. Sodabanlu, K. Watanabe, M. Sugiyama, and Y. Nakano, "Optimized interfacial management for InGaAs/GaAsP strain-compensated superlattice structure," *J. Cryst. Growth*, vol. 370, no. 1, pp. 157–162, May 2013.
- [16] K. Muraki, S. Fukatsu, Y. Shiraki, and R. Ito, "Surface segregation of atoms during molecular beam epitaxy and its influence on the energy levels in InGaAs/GaAs quantum wells," *Appl. Phys. Lett.*, vol. 61, no. 5, pp. 557–559, Aug. 1992.
- [17] L. H. Duan et al., "Fabrication and characteristics of high speed InGaAs/GaAs quantum-wells superluminescent diode emitting at 1053 nm," *Semicond. Sci. Technol.*, vol. 29, no. 5, Apr. 2014, Art. no. 055004.
- [18] S. Chen et al., "InAs/GaAs quantum-dot superluminescent lightemitting diode monolithically grown on a Si substrate," *ACS Photon.*, vol. 1, no. 7, pp. 638–642, Sep. 2014.
- [19] D. Jung et al., "Highly reliable low-threshold InAs quantum dot lasers on onaxis (001) Si with 87% injection efficiency," *ACS Photon.*, vol. 5, pp. 1094–1100, Jan. 2018.
- [20] P. K. Basu, B. Mukhopadhyay, and R. Basu, *Semiconductor Laser Theory*. CRC Press, USA: Taylor & Francis Group, LLC, 2016, pp. 234–235.
- [21] M. Kuznetsov, F. Hakimi, R. Sprague, and A. Mooradian, "Design and characteristics of high-power (0.5-WCW) diode-pumped vertical external cavity surface-emitting semiconductor lasers with circular TEM₀₀ Beams," *IEEE J. Sel. Topics Quantum Electron.*, vol. 5, no. 3, pp. 561–573, May/Jun. 1999.
- [22] M. -L. Ma et al., "Measurement of gain characteristics of semiconductor lasers by amplified spontaneous emissions from dual facets," *Opt. Exp.*, vol. 21, no. 8, pp. 10335–10341, Apr. 2013.
- [23] T. Takagi, "Refractive index of Ga_xIn_{1-x}As prepared by vapor-phase epitaxy," *Japanese J. Appl. Phys.*, vol. 17, no. 10, pp. 1813–1817, Oct. 1978.
- [24] M. S. Alam, M. S. Rahman, M. R. Islam, A. G. Bhuiyan, and M. Yamada, "Refractive index, absorption coefficient, and photoelastic constant: Key parameters of InGaAs material relevant to InGaAs-based device performance," in *Proc. IEEE 19th Int. Conf. Indium Phosphide Related Mater.*, 2007, pp. 343–346.
- [25] H. Yu, C. Roberts, and R. Murray, "Influence of indium segregation on the emission from InGaAs/GaAs quantum wells," *Appl. Phys. Lett.*, vol. 66, no. 17, pp. 2253–2255, Feb. 1995.